A Coupled Vehicle-Signal Control Method at Signalized Intersections in Mixed Traffic Environment

Yu Du, *Member, IEEE*, Wei ShangGuan, *Member, IEEE*, and Linguo Chai, *Member, IEEE*

***Abstract*—Signalized intersections play a vital role in addressing the issue of transportation efficiency and vehicle fuel economy in urban areas. Meanwhile, with the development of Connected and Automated Vehicles (CAVs), the mixed traffic environment composed of traffic participants with differing intelligent levels will become an important stage of the intelligent transportation system. Considering the changes in the mixed traffic environment, this paper proposes a Coupled Vehicle-Signal Control (CVSC) method to optimize the traffic signal timing and driving trajectories of CAVs at the same time, with the goals of traffic efficiency improvement and energy saving respectively. The signal timing is continuously optimized to minimize the total delay at the intersection. CAVs generate eco-driving trajectories using the received signal timing information and the planned arrival time to reduce fuel consumption. Finally, simulation experiments were been carried out to verify the control effect of the proposed CVSC. On the one hand, the influence of the involved parameters on the optimization results was analyzed and discussed. On the other hand, the proposed CVSC method was compared with the traditional CACC control and the classic eco-driving model, GlidePath. The research results show that the proposed CVSC method can effectively improve the performance of signalized intersections. When the penetration rate of CAVs is greater than 40%, this method can save fuel consumption by 6%-14% and increase the average speed by 1%-5%.**

***Index Terms*—Connected and automated vehicle, cooperative vehicle infrastructure control, eco-driving trajectory, mixed traffic flow, signalized intersection optimization.**

I. Introduction

THE RAPID development of urban transportation systems has brought great convenience to people's daily lives, but at the same time, it has also brought problems such as traffic congestion and energy consumption. According to a study on the actual situation of motorists in the largest cities in the United States from Texas A&M Transportation Institute, in 2017, a commuter wasted nearly seven full working days of additional traffic delays on average [1]. In terms of environmental sustainability, according to the U.S. Environmental Protection Agency [2], the transportation sector has become one of the largest contributors to greenhouse gas (GHG) emissions, accounting for 28%. Traffic mobility and sustainability are affected by many factors, such as road bottlenecks, bad weather, and traffic accidents. Among these factors, the signalized intersection plays a vital role because the stop-start wave phenomenon of vehicles leads to an increase in traffic congestion and therefore energy consumption.

In recent years, the Connected Automated Vehicle (CAV) technology is undergoing rapid development [3], [4]. CAVs can share information with other connected traffic participants, such as intelligent traffic infrastructures and other connected vehicles. Because CAVs can obtain more environmental information, such as the speed of the preceding vehicle (via Vehicle to Vehicle technology) and traffic signal timing (via Vehicle to Infrastructure technology), it has the potential to improve safety, reduce congestion, and save energy. At the same time, the coexistence of vehicles with differing intelligent levels, such as human-driven vehicles (HDVs) and CAVs, is constituting a new type of mixed traffic environment [5]. The mixed traffic environment is an important next step for intelligent transportation systems to transit from fully manual to fully automated driving.

The optimization of the signalized intersection has been a question of great interest. Considering the changes in the traffic environment, it is possible to improve the traffic performance of signalized intersections by using the above advantages of CAVs. For a long time, traffic signal optimization and vehicle trajectory optimization were usually regarded as two independent research problems. In the transportation field, traffic signal optimization has been an extensively studied area with rapid innovation to keep up with the increasing traffic demands [6]. Typically, researchers take traffic signal control as an optimization problem under certain assumptions about traffic models [7], [8], such as the well-known adaptive traffic signal controllers, SCOOT or SCATS [9], [10]. These years, learning policy from data using an artificial intelligent method such as reinforcement learning has also been widely studied to overcome non-linearity and randomness of traffic systems [11]–[14]. In term of the eco-driving at signalized intersections, researches mainly focused on vehicle trajectory generation algorithms [15], [16]. Altan *et al.* [17] proposed the GlidePath eco-driving trajectory

Manuscript received September 1, 2020; revised December 16, 2020 and January 22, 2021; accepted January 27, 2021. Date of publication February 3, 2021; date of current version April 2, 2021. This work was supported by the National Key Research and Development Program of China under Grant 2018YFB1600600. The review of this article was coordinated by Prof. V. Cerone. *(Corresponding author: Wei ShangGuan.)*

Yu Du and Linguo Chai are with the School of Electronic and Information Engineering, Beijing Jiaotong University, Beijing 100044, China (e-mail: duyu_a@bjtu.edu.cn; lgchai@bjtu.edu.cn).

Wei ShangGuan is with the School of Electronic and Information Engineering, State Key Laboratory of Rail Traffic Control and Safety, and Beijing Engineering Research Centre of EMC and GNSS Technology for Rail Transportation, Beijing Jiaotong University, Beijing 100044, China (e-mail: wshg@bjtu.edu.cn).

Digital Object Identifier 10.1109/TVT.2021.3056457

optimization method, which modelled the trajectory of the vehicle passing through the intersection as a piecewise trigonometric function. It can generate smooth vehicle trajectory and ensure the continuity of speed, acceleration, and boundedness of acceleration changes. Wang [18] proposed a collaborative energy-saving driving method based on GlidePath, which defined CAVs as 'leader' and 'follower'.

Different from the researches that only consider one-side optimization, many researchers take the coupling of vehicles and traffic signal controllers into consideration. Lee and Park [19] proposed a strategy to replace traditional traffic lights under the environment of the connected vehicle, which improved intersection throughput and reduced fuel consumption and CO2 emission. Ali *et al.* [20] applied the back-pressure algorithm, which was originally used in communication networks, to control traffic lights and reroute vehicles adaptively. Further, Yunwen *et al.* [21] proposed a game-theoretic approach to optimize signal timing and vehicle routing at the same time. Xu *et al.* [22] proposed a cooperative control method consists of two levels. The former applied the enumeration method to optimal traffic signal timing and the latter applied the pseudospectral method to calculate the engine power and brake of individual vehicles. However, little attention has been paid to the cooperative vehicle-signal optimization in a mixed traffic environment.

To sum up, from the perspective of traffic signal optimization and vehicle eco-driving method, a large number of outstanding researches have gradually matured, but the study on cooperative operation methods at signalized intersections is still limited. Especially, the existing methods which rely on pre-established rules for the allocation of temporal and spatial resources [23], [24], lack the analysis of the characteristics of random mixing of HDVs and CAVs, incapable of being directly applied in the mixed traffic environment. Inspired by the above points, this paper proposes a Coupled Vehicle-Signal Control (CVSC) method which consists of two components: traffic signal optimization and vehicle eco-driving trajectory control at signalized intersections. The contribution of the proposed CVSC method can be summarized as the following three points:

1) The proposed CVSC method aims to achieve signal-vehicle cooperation at a signalized intersection. At the macro level, the traffic signal is optimized to minimize vehicles' delay time, and at the micro-level, the CAV trajectory is optimized to save fuel consumption.
2) The analysis of the characteristics of random mixing of HDVs and CAVs which is more complicated than the pure traffic flow is taken into consideration [25]–[27]. The parameters such as saturation volume and saturation velocity are calculated based on the local CAV's penetration rate (PR) rather than the global PR.
3) Compared with traditional eco-driving methods, CVSC uses the real-time traffic information to predict the earliest departure time of CAV's at the intersection and use it as the planned arrival time to further reduce the impact of stop-start waves.

This paper is structured as follows. In Section II, the problem studied and the basic assumptions in the paper are introduced. Section III derives the fundamental diagram model of mixed traffic flow. Based on the model analyzed in Section III, Section IV presents the methodology of CVSC, including traffic signal optimization and CAV eco-driving control model. The simulation and results are presented in Section V. Finally, in Section VI we present our conclusion.

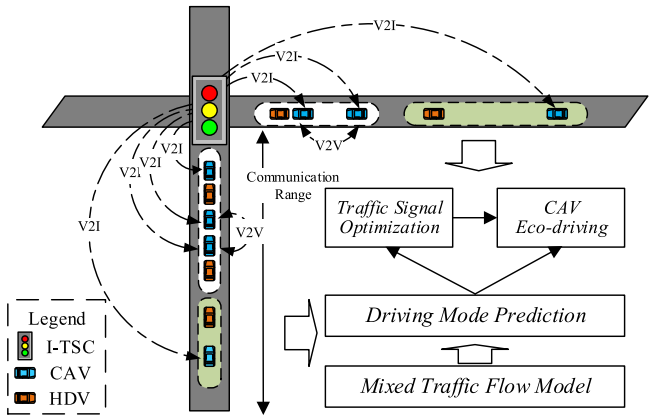

Fig. 1. Illustration of the proposed coupled vehicle-signal control system.

II. Problem Statement

The objective of this study is to develop a coupled vehicle-signal control system to improve operating efficiency and reduce energy consumption at signalized intersections on the premise of ensuring safety. Utilizing the V2I and V2V communication, the proposed CVSC method collaborative control the CAVs and Intelligent Traffic Signal Controllers (I-TSCs) in a mixed traffic environment. The mixed traffic environment consists of three participants: HDVs, CAVs, and I-TSCs, as shown in Fig. 1.

On the one hand, I-TSC perceives the status information of vehicles approaching the intersection area and calculates a set of green light time to minimize the total delay of all vehicles. The method of obtaining vehicle information is out of the scope of this article because it is known that it can be achieved by several methods such as sensor fusion [28]. One possible way is to combine the sensing data from a camera and V2I. I-TSC can obtain the location information of all nearby vehicles through the equipped camera, and use communication technology to receive all CAVs' message. Through the matching of the two kinds of data, I-TSC can obtain the real-time status of nearby vehicles and distinguish the vehicle type (HDV or CAV).

On the other hand, CAVs execute the trajectory control algorithm according to whether the eco-driving control conditions are met. When the CAV enters the communication range of the I-TSC, it will send its location and route selection to the I-TSC, and receive the signal settings sent by the I-TSC. If the eco-driving conditions are met, the CAV will automatically calculate and execute the optimized driving speed trajectory according to the planned best arrival time to minimize vehicle fuel consumption. Otherwise, its original car-following model will be executed. In addition, HDVs are not controlled by the system but will affect the entire traffic flow.

Traffic signal optimization updates the signal timing plan cycle by cycle according to the real-time information of all

approaching vehicles. A set of green time for all phases is calculated to minimize the delay time of all vehicles by estimating the number of vehicles that can pass through the intersection based on the fundamental diagram model. Vehicle eco-driving trajectory control is applied to CAVs which meet re-planning conditions to save fuel consumption for the entire traffic flow. Different from the existing work, the trajectory of CAVs is based on the planned arrival time, which involved not only the traffic signal information but also the status of other vehicles ahead. Here we give some assumptions which will be relied on for the CVSC method:

1) Vehicle lane changing and overtaking have been done before they enter the intersection area.
2) Factors such as delays and packet loss during communication are not considered.
3) The difference in driver driving style is not taken into account, therefore the same parameters are applied to HDVs.
4) The influence of factors on fuel consumption is not taken into account, such as changes in air resistance caused by different driving sequences.

III. Fundamental Diagram Model of Mixed Traffic Flow

The fundamental diagram model of mixed traffic flow is used for judging the driving mode of vehicles, which is the basis for decision-making in the CVSC method. In this section, we will first introduce the mixed traffic flow model involved in the algorithm. The specific algorithm will be detailed in Section IV.

A. Car Following Model

1) Intelligent Driver Model: The Intelligent Driver Model (IDM) [29] proposed by Treiber is chosen to describe the car-following behavior of HDVs, as Eq. (1). a_n and v_n are the acceleration and velocity of the ego vehicle, respectively. v_f is the free flow velocity. $\triangle v_n$ and $\triangle x$ are the speed and position difference between the ego vehicle and the preceding vehicle, $\triangle v_n = v_{n-1} - v_n$, $\triangle x_n = x_{n-1} - x_n$. L is the length of vehicles. s_0 is the minimum distance between vehicles. T is the safe time headway which depends on the driver's reaction time; a and b are the maximum acceleration and comfortable deceleration of the vehicle, respectively.

$$\begin{cases} a_n = a\left[1 - \left(\dfrac{v_n}{v_f}\right)^4 - \left(\dfrac{s^*(v_n, \triangle v_n)}{\triangle x - L}\right)^2\right] \\ s^*(v_n, \triangle v_n) = s_0 + v_n T + \dfrac{v_n \triangle v_n}{2\sqrt{ab}} \end{cases} \tag{1}$$

The value of parameters are taken from [29], and are $s_0 = 2\,m, L = 5\,m, T = 1.6\,s, a = 0.73\,m/s^2, b = 1.67\,m/s^2$. Considering that the scenario in this paper is the signalized intersection of an urban road, the free flow velocity is set to $16\,m/s$.

2) Cooperative Adaptive Cruise Control: The Cooperative Adaptive Cruise Control (CACC) [30], [31] model was developed by PATH Labs and calibrated based on real vehicle trajectory data, and it is widely used to describe the following behavior of CAVs, as shown in Eq. (2–3). e is the error between the actual distance and the expected distance; $\dot{e}$ is the differential of the error term e; t_c is the desired time headway, k_p and k_d is the model control parameter; $\triangle t$ is the control interval. Refer to the calibration in [31], the parameters are $k_p = 0.45\,s^{-1}, k_d = 0.25, t_c = 0.6, \triangle t = 0.01\,s$.

$$\begin{cases} v_n = v_{n-1} + k_p e + k_d \dot{e} \\ e = \triangle x - s_0 - L - t_c v_n \end{cases} \tag{2}$$

$$a_n = \frac{k_p(\triangle x - s_0 - L - t_c v_n) + k_d \triangle v_n}{k_d t_c + \triangle t} \tag{3}$$

3) Adaptive Cruise Control: If a CAV follows an HDV, the car following model of the CAV will automatically transform from CACC to Adaptive Cruise Control (ACC) [31], due to the lack of vehicle communication equipment in HDVs [32]. The control model of ACC is shown as Eq. (4). k_1, k_2 are control parameters and t_a is the expected time headway. According to the calibration results of PATH, $t_a = 1.1\,s, k_1 = 0.23\,s^{-2}$ and $k_2 = 0.07\,s^{-1}$.

$$a_n = k_1(\triangle x - s_0 - L - t_a v_n) + k_2 \triangle v_n \tag{4}$$

B. Fundamental Diagram Model of Mixed Traffic Flow

The fundamental diagram model of mixed traffic flow can be obtained through the stable space headway. Set the speed difference and acceleration value in Eq. (1), Eq. (3) and Eq. (4) to zero, then the stable space headway at the steady state can be obtained, as shown in Eq. (5–7).

$$h_r = \frac{s_0 + vT}{\sqrt{1 - (v/v_0)^4}} + L \tag{5}$$

$$h_a = vt_a + L + s_0 \tag{6}$$

$$h_c = vt_c + L + s_0 \tag{7}$$

Assuming that there are N vehicles in the traffic flow and the penetration rate of CAVs is $p(0 \le p \le 1)$. Then, the number of HDVs is $N(1-p)$, and the number of CAVs is Np. The proportion of CAV degenerating to the ACC model is Eq. (8) and the proportion of CAV running CACC model is Eq. (9).

$$N(1-p)\frac{Np}{N} = N(1-p)p \tag{8}$$

$$Np - N(1-p)p = Np^2 \tag{9}$$

Therefore, when the penetration rate of the CAV vehicle is p, the actual proportion of CACC model, ACC model, and IDM respectively are p_a, p_c, and p_r, as calculated in Eq. (10).

$$p_c = p^2, p_a = p(1-p), p_r = 1 - p \tag{10}$$

The average space headway of the mixed traffic flow at steady state can be calculated as Eq. (11). Then, according to to the relationship between vehicle speed, volume and density of

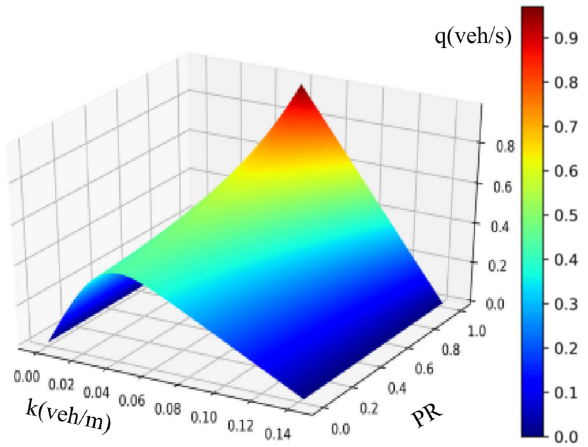

Fig. 2. The fundamental diagram model of mixed traffic flow.

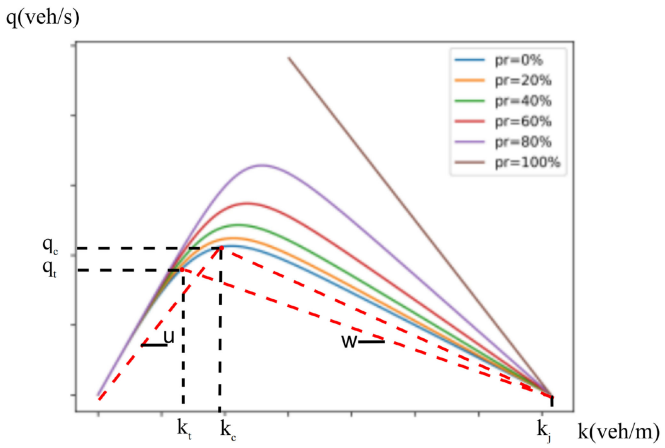

Fig. 3. The fundamental diagram model of mixed traffic flow under partial PR conditions.

traffic flow, the density of mixed traffic flow and volume can be calculated by Eq. (12) and Eq. (13) respectively.

$$h^* = p_c * h_c + p_a * h_a + p_r * h_r \tag{11}$$

$$k^* = \frac{1}{p_c * h_c + p_a * h_a + p_r * h_r} \tag{12}$$

$$q^* = k^* v = v/(p^2(vt_c + L + s_0) + p(1-p)(vt_a + L + s_0) + (1-p)(\frac{s_0 + vT}{\sqrt{1-(v/v_0)^4}} + L)) \tag{13}$$

The fundamental diagram model of mixed traffic flow is illustrated in Fig. (2). And Fig. (3) shows the relationship between volume and density under partial PR conditions. q_c is the saturated volume which is the maximum volume that can be reached given a specific PR condition, and its corresponding density is the saturated density k_c. As the proportion of CAV in the traffic flow increases from 0 to 1, the maximum volume also gradually increases, which represents that CAVs can effectively increase the capacity of the existing transportation system.

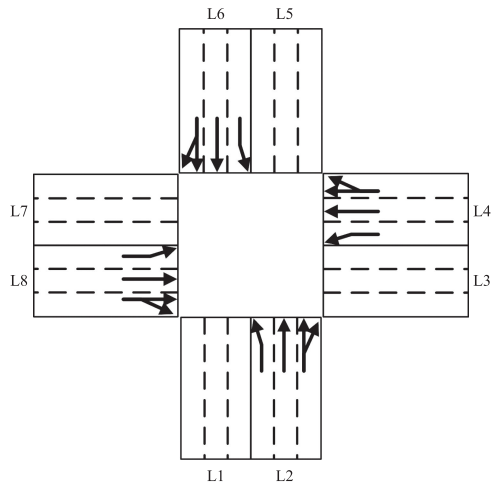

Fig. 4. A typical four-way intersection with 8 roads and 12 routes.

IV. Coupled Vehicle-Signal Control

The CVSC method uses the fundamental diagram model of mixed traffic flow as the connection for achieving the coordinated control of both ends of I-TSCs and CAVs at signalized intersections, with the goals of efficiency and energy saving respectively.

In terms of efficiency, I-TSC predicts the number of vehicles that can pass through the intersection in a given green light time to optimize signal timing. In terms of energy saving, different from the existing methods, the CVSC method takes into account the starting time required for the stopped vehicles and HDVs in front of the CAVs and calculate the planned arrival time to avoid the unnecessary parking and save energy. First, put forward two assumptions on which this section is based:

1) The I-TSC can sense the real-time traffic information and the types of vehicles on the upstream roads and send it to CAVs through V2I.
2) When the green light starts, vehicles in front of the stop line will pass through the intersection in saturated traffic volume.

A. Traffic Signal Optimization

We consider a typical 4-leg, 3-lane (in each direction) signalized intersection as the case to explain the traffic signal optimization method. As shown in Fig. 4, there are 8 roads at the intersection, denoted as $L1$-$L8$. Also, there are 12 routes according to the possible traffic demand without considering turning around, which can be denoted as $R_{ab} \in \mathbb{R} = \{R_{23} = (L2 \to L3),\ R_{25} = (L2 \to L5),\ R_{27} = (L2 \to L7),\ R_{41} = (L4 \to L1),\ R_{45} = (L4 \to L5),\ R_{47} = (L4 \to L7),\ R_{61} = (L6 \to L1),\ R_{63} = (L6 \to L3),\ R_{67} = (L6 \to L7),\ R_{81} = (L8 \to L1),\ R_{83} = (L8 \to L3),\ R_{85} = (L8 \to L5)\}$.

The traffic signal control cycle is predefined as C, which consists of four phases: west-east-through (WET), west-east-left turning (WEL), north-south-through (NST), and north-south-left turning (NSL). Each signal phase controls a series of routes and the through and right turn directions are regarded as the same direction. The initial fixed timing plan is shown in Table I.

TABLE I
THE PHASE SEQUENCE AND FIXED SIGNAL TIMING FOR THE INTERSECTION

Phase	Routes	Signal Timing (s)
Ph_1 (WET)	R_{47}, R_{83}	18 2
Ph_2 (WEL)	R_{41}, R_{85}	18 2
Ph_3 (NST)	R_{25}, R_{61}	2 18 2
Ph_4 (NSL)	R_{27}, R_{63}	18 2

The green time of the ith phase is denoted as T_{gi} which is the green duration of a set of routes R_{ab}.

The purpose of signal timing optimization is to find a set of green time that minimizes all the vehicles' delay. The cost function is defined as Eq. (14–17). Z_i represents the time required for all the delayed vehicles controlled by phase Ph_i to pass through the intersection. It can be seen that the cost function consists of two parts with the weight parameters, w_1 and w_2. The first part minimizes the delay time for all delayed vehicle, and the second part minimizes the difference among all phases to ensure fairness.

$$\min_{\{Tg\}} \theta = w_1 * \frac{1}{4}\sum_{i=1}^{4} Z_i + +w_2 * \sum_{i=1}^{4}\left(\frac{1}{4}\sum_{j=1}^{4} Z_j - Z_i\right)^2 \tag{14}$$

$$Z_i = \tau \times S_i \tag{15}$$

$$\tau = \frac{h^*}{v_c} \tag{16}$$

$$S_{ab} = N_{ab} - P_{ab} \tag{17}$$

N_{ab} is the total number of vehicles at the route R_{ab}, and P_{ab} is the number of vehicles that can be served within the current green time. S_{ab} is the number of delayed vehicles. S_i is the maximum value among all the R_{ab} controlled by the phase Ph_i. τ is the average time headway of the traffic flow, which can be calculated by dividing average space headway h^* by saturated speed v_c. And the variable T_{gi} to be solved is the green time allocated to phase Ph_i at the next control cycle. The solution of T_{gi} is constrained by the following conditions (18), where T_{gmin} and T_{gmax} are the minimum and maximum green time, respectively.

$$s.t. \begin{cases} \sum_{i=1}^{4} T_{gi} = C \\ T_{gi} \geq T_{gmin},\ T_{gi} \leq T_{gmax} \\ S_i \geq S_{ab},\ R_{ab} \rightarrow Ph_i \end{cases} \tag{18}$$

In order to accurately estimate the value P_{ab}, the vehicles that can be served within the green time is predicted based on the real traffic status. The departure process of the stopped vehicles and the arriving HDVs will cause the stop-start wave when the green time starts. The first non-stop arriving CAV on upstream traffic flow is denoted as the First-CAV. Fig.(5) shows an example to illustrate the involved values. Assuming that the First-CAV is the Kth vehicle before the stop line of the intersection, and the distance to the intersection is D_k. X_Q is the length of queued vehicles already existing at the intersection. T_g is the green time of the phase. T_r is the remaining red time before the green light starts. X_{max} and N_{max} respectively are the possible maximum distance and vehicle number can be served, as Eq. (19)–(20).

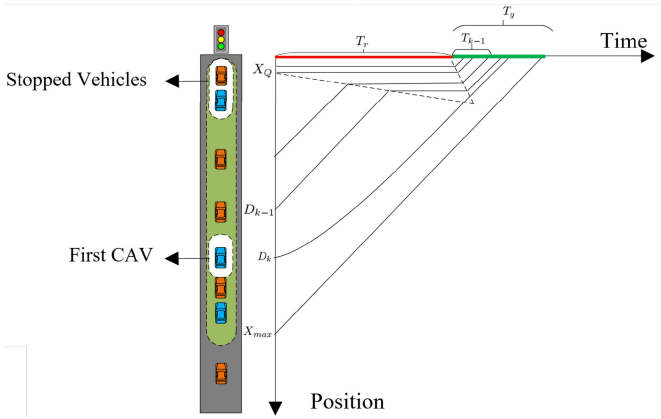

Fig. 5. Vehicle trajectory evolution in the time-space domain at a signalized intersection.

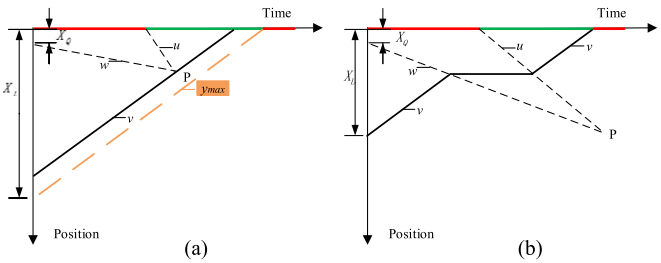

Fig. 6. The calculation of the value X_L.

$$X_{max} = (T_r + T_g) \times v_f \tag{19}$$

$$N_{max} = T_g \times v_c^*/h^* \tag{20}$$

Then the number of vehicles that can be served is estimated according to Eq. (21). If the distance from the First-CAV to the intersection is larger than the possible maximum service distance X_{max} or the preceding vehicle (the $(K-1)th$ vehicle) cannot pass the intersection in the green time T_g, the service distance will depend on the number of vehicles in the distance X_L. Otherwise, P_{ab} equals the minimum value of the number of vehicles in X_{max} and N_{max}. The function $Count(a, b)$ represents counting the number of vehicles whose distance to the intersection is between a and b. Similarly, $CountCAV(a, b)$ represents counting the number of CAVs within the distance from a to b.

$$P_{ab} \begin{cases} Count(0, X_L), & \text{if } T_{k-1} > T_g \text{ or } D_k > X_{max} \\ \min(Count(0, X_{max}), N_{max}), & \text{else} \end{cases} \tag{21}$$

The value of X_L is derived from the fundamental diagram model, which is illustrated in Fig. (6). The dotted black line represents the propagation path of the stop wave and the start

wave. Establish a coordinate system as Fig. (6), by solving the geometric relationship in the figure, the position of point P an be calculated as Eq. (22–23). According to the linear programming method, bring P_x into the function y_{max}, and record the result as P'_y. If $P'_y < P_y$, it conforms to the condition shown in Fig.(6(a)), where the wave impact ends before the green time ends. The value of X_L and T_{k-1} are calculated as Eq. (24). Otherwise it conforms to the condition in Fig.(6(b)), then the wave impact continues after the green time ends. The value of X_L and T_{k-1} are calculated as Eq. (25). q_t, k_t and v_t are the volume, density, and vehicle speed of the upstream traffic flow before red light starting; k_j is the congestion density, that is, the traffic density when parking; q_c and k_c are the saturated flow and saturated density corresponding to the PR on the lane. u and w respectively are the start wave speed and the stop wave speed, as Eq. (26–28), which are derived from the fundamental diagram model as Fig. 3.

$$P_x = \frac{X_Q + uT_r}{u - w},\ P_y = \frac{uX_Q + uwT_r}{u - w} \tag{22}$$

$$y_{max} = -v(x - T_r - T_g) \tag{23}$$

$$\begin{cases} X_L = X_{max} \\ T_{k-1} = \dfrac{P_y}{v} + P_x \end{cases} \tag{24}$$

$$\begin{cases} X_L = \dfrac{T_g uv}{u + v}\left[1 + \dfrac{v}{w}\right] - v\dfrac{X_Q}{w} \\ T_{k-1} = T_g \end{cases} \tag{25}$$

$$u = \frac{q_c}{k_c} \tag{26}$$

$$w = \frac{q_t}{k_t - k_j} \tag{27}$$

$$q_t = \begin{cases} q_c\ if\ k_t \geq k_c \\ v_t \times kt\ else \end{cases} \tag{28}$$

At the beginning of a new traffic signal cycle, the traffic signal timing plan for the next cycle is calculated by the I-TSC. The sequential least squares programming (SLSQP) optimizer is applied to solve the optimization problem of Eq. (14). The fixed timing plan mentioned in Table I is set as the initial value for the optimizer.

B. CAV Eco-Driving Trajectory Generation

1) Planned Arrival Time: First, introduce the meaning of the variables involved in this chapter. d_0 is the distance between the vehicle to the intersection. S is the current state of the traffic light. D_c is the communication range. T_{lgt} is the remaining green time, when the light state is red, $T_{lgt} = T_g$. T_{rgt} is the remaining time to the next green time, when the light state is green, $T_{rgt} = 0$. The PR value of traffic flow is a macro parameter, which is relatively stable for the entire traffic flow. However, because the traffic flow at signalized intersections is discontinuous, it is the local PR that affects the ego vehicle, which depends on the vehicles between the ego vehicle and the stop line. Therefore the variable p^n is proposed as the local PR for the Nth CAV, as Eq. (29).

TABLE II
THE DIFFERENCE OF PLANNED ARRIVAL TIME AND THE DEPARTURE TIME COLLECTED IN CAR-FOLLOWING MODE

PR	Avg. Diff(s)	Max. Diff(s)
0	0.15	0.15
0.2	0.35	0.76
0.4	0.22	0.32
0.6	0.43	0.56
0.8	0.31	0.45
1.0	0.17	0.18

$$p^n = \frac{CountCAV(0, d_0)}{N} \tag{29}$$

Assuming that an ego CAV is the Nth vehicle on the upstream road, if it satisfied $d_0 < D_c$, it will judge whether the trajectory needs to be re-planned every time interval (set to 2 s). If a CAV satisfies the following two conditions, an eco-driving speed curve will be generated:

1) $S = green\ \&\ N \times h^n / v_c^n < T_{lgt}\ \&\ d_0 \leq N \times h^n$: The CAV can pass through the intersection within current green time.
2) $S = red\ \&\ N \times h^n / v_c^n < T_g\ \&\ d_0 < (T_g + T_r) \times v_f$: The CAV can pass the intersection in the next green time.

For avoiding the formation of deceleration waves, the time when the vehicle departs from the intersection in car-following model is estimated and applied as the planned arrival time. Combining the relationship between the volume, density and space headway, the planned arrival time of the ego CAV, t_{arr}, is calculated as Eq. (30–32). h^n is the estimated average space headway, and v_c^n is the estimated saturation speed. q^{p^n} is the saturation volume, which is solved by bring the Eq. (29) into Eq. (13).

$$t_{arr} = \frac{N \times h^n}{v_c^n} + T_{rgt} \tag{30}$$

$$h^n = N((p^n)^2 h_c + p^n(1 - p^n)h_a + (1 - p^n)h_r) \tag{31}$$

$$v_c^n = \max_v q^{p^n} \tag{32}$$

Table II shows the difference between the planned arrival time calculated by the eco-driving algorithm and the time when the vehicle departs from the intersection in car-following mode. It can be seen that the difference is less than 1 s with PR ranging from 0 to 1. Fig.(7) shows the comparison of planned arrival time calculated by CVSC and the departure time collected in car-following mode under the condition of $PR = 0.5$. The blue curve is the CAV driving trajectory; the yellow curve is the HDV driving trajectory; the green mark is the planned arrival time, and the red mark is the departure time obtained from the simulation experiment. The results show that the planned arrival time is very close to the time the vehicle departs from the intersection in the car-following mode.

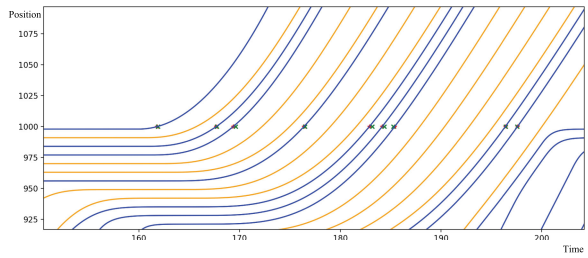

Fig. 7. The difference of planned arrival time calculated by CVSC and the departure time collected in car-following mode.

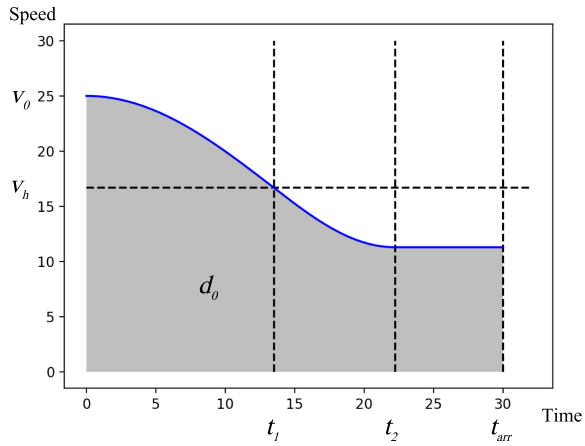

Fig. 8. Trajectory generation algorithm based on piecewise trigonometric function.

2) CAV Longitudinal Control: The driving strategy adopted by CAV is to decelerate (or accelerate) to a constant speed first, then pass the intersection with the constant speed. Inspired by GlidePath [17], the acceleration control strategy based on trigonometric function is selected. This method can guarantee the continuity of speed and acceleration, also the boundedness of acceleration changes. The trajectory profile is shown in Fig. (8). The blue curve is the target speed of the vehicle, and the area enclosed by the x-axis is the distance from the CAV to the intersection.

The speed curve is divided into three parts. In the first part, the deceleration of the vehicle gradually increases, and the vehicle speed decreases from the initial speed v_0 to the average speed v_h. In the second part, the deceleration of the vehicle gradually decreases to 0, the vehicle speed decreases from the average speed v_h to a constant speed. At last, the acceleration is 0, and the vehicles pass through the intersection with a constant speed. The speed curve of these three stages can be represented as Eq. (33–37). After passing the intersection, the driving model of CAV will go back to the original control model, CACC or ACC. If $v_0 < v_h$, the vehicle will first accelerate, and the acceleration process is exactly as same as the deceleration.

$$v_t = \begin{cases} v_h - v_d \cos(mt) & t \in [0, t_1) \\ v_h - v_d \dfrac{m}{n} \cos\left(n\left(t + \dfrac{\pi}{n} - t_2\right)\right) & t \in [t_1, t_2) \\ v_h + v_d \dfrac{m}{n} & t \in [t_2, t_{arr}) \end{cases} \tag{33}$$

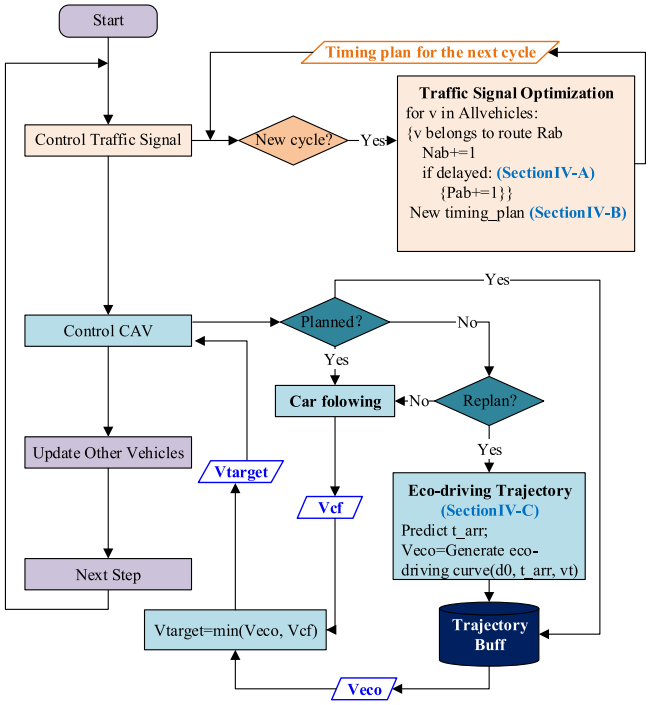

Fig. 9. The whole procedure of CVSC method.

$$t_1 = \frac{\pi}{2m} \tag{34}$$

$$t_2 = \frac{\pi}{2m} + \frac{\pi}{2n} \tag{35}$$

$$v_h = \frac{d_0}{t_{arr}} \tag{36}$$

$$v_d = v_h - v_0 \tag{37}$$

m and n are the control parameters to ensure the smoothness of the piecewise trigonometric function. m is calculated as Eq. (39) and n is the largest positive number that satisfies the constraints in Eq. (38), where a_{max} is the maximum acceleration, d_{max} is the maximum deceleration, and $jerk_{max}$ is the maximum first time derivative of acceleration.

$$J(n) = \begin{cases} |nv_d| \le a_{max} \\ |nv_d| \le d_{max} \\ |n^2 v_d| \le jerk_{max} \\ n \ge \left(\dfrac{\pi}{2} - 1\right) \cdot \dfrac{v_h}{d_0} \end{cases} \tag{38}$$

$$m = \frac{-\dfrac{\pi}{2}n - \sqrt{\left(\dfrac{\pi}{2}n\right)^2 - 4n^2\left[\dfrac{\pi}{2} - 1 - \dfrac{d_0}{v_h}n\right]}}{2\left[\left(\dfrac{\pi}{2} - 1\right) - \dfrac{d_0}{v_h}n\right]} \tag{39}$$

C. The Whole Procedure

The whole procedure of CVSC method is illustrated in Fig.(9). When a new traffic signal control cycle C_T starts, the Traffic

Signal Optimization component is started to generate the timing plan for the next cycle, C_{T+1}. The number of vehicles that can pass through the intersection are predicted, as introduced in Section IV-A. The remaining vehicles are predicted as delayed vehicles. A set of green time for the cycle C_{T+1} is calculated as the solution to minimize the total delay of all delayed vehicles in the communication range.

CAVs entering the communication range of I-TSC receive the traffic signal information from the I-TSC continuously and judge their driving mode every control interval. If the CAV has not been planned and it meets the re-plan condition, an eco-driving speed curve will be generated based on the current position, speed and planned arrival time. The eco-driving speed curve is stored onboard. Every vehicle control interval, the car following model (CACC or ACC) calculates a car following speed V_{cf}, which is considered as the safety constraint to avoid collisions. If CAV has planned an eco-driving speed curve, the current eco-speed V_{eco} will be obtained from the memory, else $V_{eco} = V_{max}$. The target speed is the smaller one of the car following speed V_{cf} and eco-driving speed V_{eco}. The purpose of the eco-driving algorithm is to make CAVs no longer need to fully stop in front of the stop line and avoid the formation of deceleration waves at the intersection. At other times, vehicles autonomously execute their own control strategy and HDV keeps its own car-following model.

V. Simulation and Discussion

A. Simulation Settings

To verify the proposed CVSC method and evaluate its system-wide performance, we conducted simulation with open source traffic simulation software SUMO [33]. The Handbook Emission Factors for Road Transport model (HBEFA) provided by the SUMO is used to estimate the fuel consumption and CO2 emission [34]. The simulation time of each experiment is 500 s, and the simulation step is 10 ms. The final experimental data is the average of three times of simulation under the same conditions. The intersection model in Fig.(4) is adopted, and the length of all corridors is 1500 m.

First, the CACC model and fixed time traffic signal were implemented as the baselines. The impact of key parameters in developing the CVSC were analyzed, including the communication range and traffic signal control cycle. Second, we implemented the classic eco-driving algorithm GlidePath as another baseline. The comparison of CACC, Glidepath, and the proposed CVSC were performed in terms of traffic efficiency and energy consumption. To evaluate the proposed CVSC under different conditions, two factors were considered, including the PR and the traffic volume of the mixed traffic flow. Measurements of effectiveness adopted were fuel consumption, CO2 emissions, average vehicle speed, vehicle stopped ratio and average waiting time.

B. Parameter Impact

1) Communication Range: Fig.(10) shows the average fuel consumption and vehicle delay of proposed CVSC method under different communication range. In this case, the ratio of CAV is 60% (PR = 0.6), the traffic volume is 80% of the saturated flow (the ration of volume to capacity is V/C = 0.8), and the length of a signal control cycle is 60 s. The original CACC method is used as the baseline.

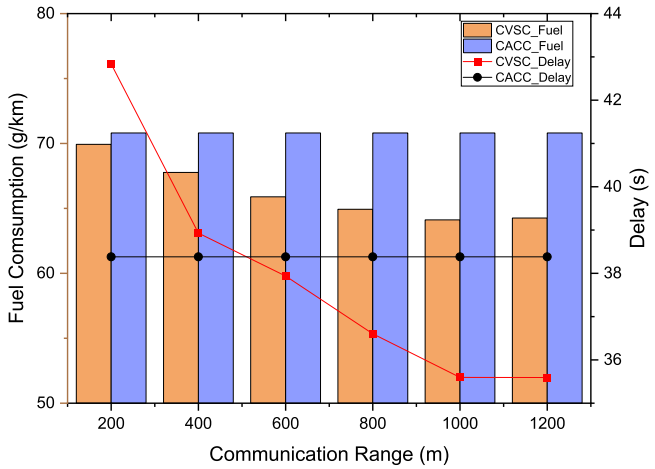

Fig. 10. The impact of communication range on average fuel consumption and vehicle delay.

As can be seen, the CVSC method always consumes less fuel than the CACC method. When the communication range is greater than 600 m, positive impacts on travel delay are shown. Generally speaking, the performance gain of the CVSC method increases as the communication range increases. When the distance is greater than 1000 m, the gain in fuel consumption and travel delay remain stable at about 9% and 7% respectively.

It is thought that there are two main reasons for this result. First, if the sensing range is too small, the knowledge of the delayed vehicles cannot be obtained by the I-TSC. Second, CAVs also need a minimum distance to change the speed control strategy. When the control cycle length is 60 s and free speed is $16\,m/s$, the sensing range which can fully meet the data requirements of traffic signal optimization is $60s \times 16\,m/s = 960\,m$. Therefore, when the communication range is above 1000 m, the vehicle delay is significantly reduced; when it is about 600m-800 m, the I-TSC seems can also achieve delay reduction relying on partial vehicle knowledge, because the average travelling speed is about $10\,m/s - 12\,m/s$. While, when the communication distance is less than 400 m, the lacking of information on arrival vehicles makes it difficult for I-TSC to obtain optimized results. Therefore, enough communication range is required by the CVSC for positive performance improvement.

2) Cycle Length: The impact of signal control cycle length on the system performance is shown in Fig.(11). In this case, PR = 0.6, V/C = 0.8, and the communication range is 800 m. There is a tendency for both of the methods that as the cycle length increases, vehicle delays and energy consumption also increase. According to the traffic flow theory, generally a longer signal cycle give rise to the increase in vehicle delay.

It can be observed that compared with the CACC method, the proposed CVSC improves traffic performance in both travel efficiency and fuel consumption. When the cycle length is less

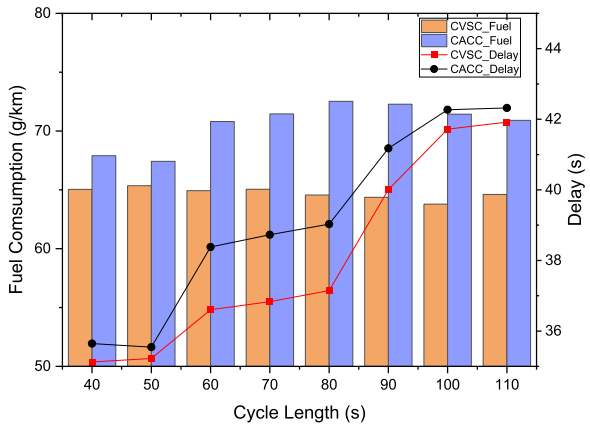

Fig. 11. The impact of signal control cycle length on average fuel consumption and vehicle delay.

than 50 s, the delay time of the two methods is basically the same. When the cycle is greater than 50 s, the CVSC method significantly reduces vehicle delay. Similar to the reason explained in the communication range experiment, when the communication distance is 800 m, the corresponding matched signal cycle is 50 s. Therefore when the signal cycle is less than 50 s, CVSC uses complete knowledge to make a decision on the next signal cycle; when the cycle is greater than 50 s and less than 80 s, the signal optimization component relies on partial knowledge. Otherwise, if the cycle is greater than 80 s, CVSC has limited advantages in efficiency improvement. In short, these results indicate that when the signal control cycle and the communication range are matched, the proposed CVSC can effectively reduce fuel consumption and vehicle delays.

C. Performance Comparison

1) Comparison of Driving Trajectory: We first conduct a simple case to intuitively show the control effects of driving trajectory using different CAV control methods. The result of the numerical experiment is shown in Fig. (12). In this case, the traffic signal timing is set as the fixed time mode, and the vehicle trajectories of three control methods are drawn, including the CVSC, classic eco-driving control method, Glidepath, and traditional CACC model. The yellow curve is the driving trajectory of HDVs, and the blue curve is CAVs. Fig.(12-(a)) and Fig.(12-(b)) show the comparison when the global PR $=$ 50% and PR $=$ 100%, respectively. Compared with the CACC model, both of the GlidePath model and the CVSC model can avoid the complete parking of vehicles. However, the GlidePath model causes obvious deceleration waves. By planing the arrival time considering the stop-start wave, the trajectories generated by the CVSC model are much smoother and can significantly reduce the impact of deceleration waves. Therefore, the proposed CVSC method has a more obvious suppression effect on the stop-start wave at the signalized intersection.

2) Impact of Penetration Rate: Here, a more comprehensive comparison experiment based on different PRs is implemented. Three kinds of models are involved: the combination of CACC and the fixed signal controller; the combination of GlidePath and the gap-based actuated traffic signal control (ASC) and the proposed CVSC model. In addition, the ASC algorithm is provided by the TraCI API of SUMO. These three methods are denoted as CACC, Glide, and CVSC respectively. In the case, V/C $= 0.8$, $C = 62\,s$, and the communication range is $800\,m$. The comparison results on fuel consumption, CO2 emission, average speed, and average waiting time with different PRs are listed in Table III. Below the column of each evaluation index, the three sub-columns respectively are the simulation results of the CACC model and the performance beneficial gains of CVSC and GlidePath+ASC compared with CACC.

For all the three methods, there is a tendency that the average speed, fuel consumption, and CO2 emissions of traffic flow increase as the proportion of CAVs increases. One reason is that the CAV has a smaller space headway therefore it is able to increase the average speed of the traffic flow. Another reason is the increase in speed requires more energy. Compared with the CACC method, remarkable improvement can be obtained by using the CVSC method, even in the case of small PR of CAVs. When the PR is larger than 0.2, about 6%-14.5% of fuel can be saved; when the PR is greater than 0.4, the average speed increases by 1%-5%. Because the CAVs can be controlled to decelerate in advance to avoid a complete stop, both of the GlidePath and CVSC can greatly reduce the waiting time and fuel consumption compared with the traditional CACC method. It is also apparent that, by taking the deceleration wave phenomenon into the consideration, the proposed CVSC method outperforms the GlidePath method in both traffic efficiency and fuel consumption.

When PR $= 0$, there is no CAV in the environment, the slight difference of the CVSC and CACC is caused by the I-TSC component. It improves the average travelling speed slightly by 0.61% and reduces the average waiting time by 4%, which leads to an increase in energy consumption by about 1%. When PR $=$ 1, all the cars in the environment are CAVs, and the performance benefit of each evaluation index reaches the maximum. The CVSC method is able to save fuel consumption and reduce CO2 emissions by about 14%. Meanwhile, the average travel speed of all vehicles increases by 5% and the vehicle waiting time is close to zero.

Fig. (13) illustrates the impact of CVSC method on different vehicles. The black, blue, and red curves represent the average waiting time of all vehicles, HDVs and CAVs, respectively. The general trend is that the increase in PR reduces the average waiting time of vehicles in the traffic flow. The result shows that when the PR is greater than 0.2, the average waiting of HDVs has dropped significantly. It could be inferred that the CVSC has a positive impact not only on the controlled CAVs but also on the other HDVs.

3) Impact of Traffic Volume: Table IV shows the comparison results of the three methods with traffic demand changing from 20% of saturated traffic volume (V/C $= 0.2$) to saturated traffic volume (V/C $= 1$). In this case, PR $= 0.6$, $C = 60\,s$, the communication range is $800\,m$, and the traffic demand on each route is balanced. The simulation results show that when the traffic demand is pretty small, the optimization effect is not obvious since there are few cars on the road. When the V/C $= 0.8$, the

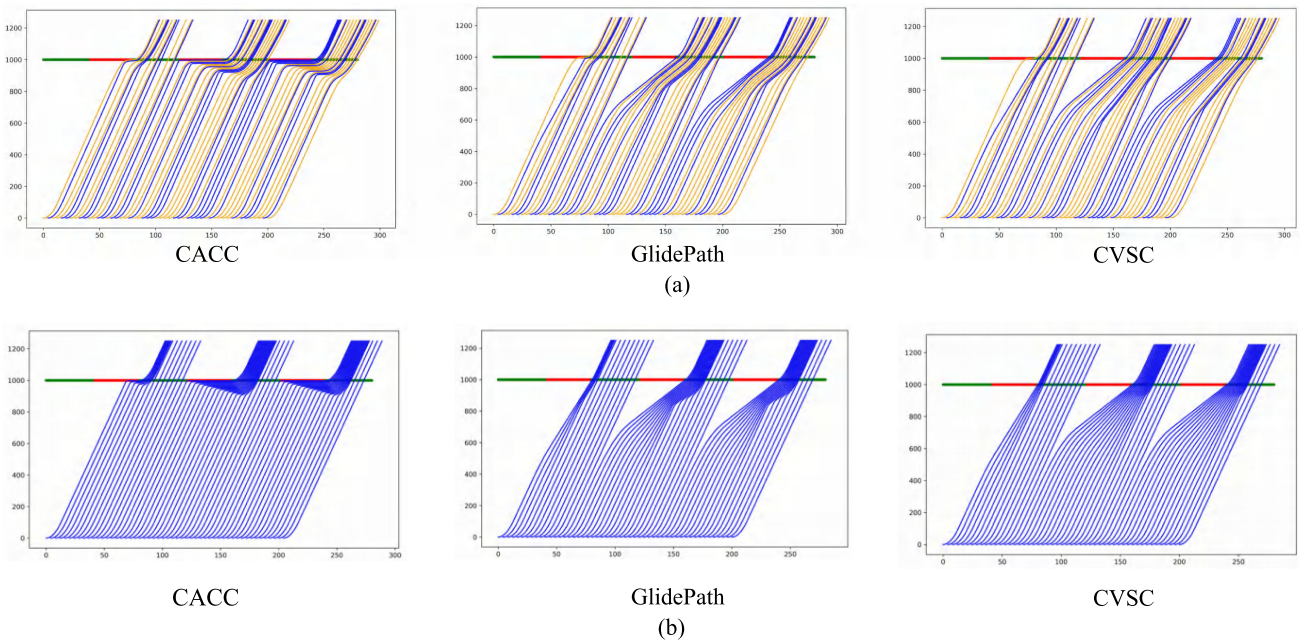

Fig. 12. Comparison of the control trajectories of CACC, GlidePath and PAT. (a) Comparison of vehicle control effect with 50% PR. (b) Comparison of vehicle control effect with 100% PR.

TABLE III
THE OVERALL PERFORMANCE OF THE TRAFFIC NETWORK AT DIFFERENT PR UNDER CACC, CVSC, AND GLIDEPATH

PR	Fuel Consumption			CO2 Emission			Average Speed			Average Waiting Time		
	Fuel (g/km)	Benefits (%)		CO2 (g/km)	Benefits (%)		Speed(m/s)	Benefits (%)		Time(s)	Benefits (%)	
	CACC	CVSC	Glide	CACC	CVSC	Glide	CACC	CVSC	Glide	CACC	CVSC	Glide
0	66.2	-1.09	-0.35	153718.62	-0.91	-0.13	10.89	0.61	0.22	12.74	4.14	0.63
0.1	67.49	3.86	0.38	156482.29	3.53	0.43	10.93	0.88	-0.34	12.61	8.4	1.62
0.2	69.42	5.91	2.23	162066.14	6.25	2.29	10.96	0.69	0.36	12.46	17.59	3.62
0.3	71.51	7.11	0.94	166394.11	7.13	2.24	11.08	0.32	0.02	11.27	35.45	3.28
0.4	66.26	6.75	1.88	153602.97	6.42	1.84	11.23	2.17	-0.35	12.02	56.73	15.97
0.5	67.47	5.85	1.52	157246.71	6.02	1.31	11.21	2.85	0.18	11.55	63.29	29.89
0.6	69.71	6.02	2.87	159839.33	4.65	2.08	11.43	1.45	0.21	10.10	65.75	22.79
0.7	70.85	7.72	5.52	160330.4	5.13	2.73	11.52	1.17	0.10	10.50	78.45	49.52
0.8	72.54	8.52	5.84	168655.67	11.12	3.86	11.58	4.41	0.81	9.95	76.20	48.72
0.9	76.49	13.57	6.20	174061.26	13.94	3.12	11.63	4.65	1.78	9.46	76.36	49.28
1	78.01	14.47	6.36	182006.63	13.95	3.82	11.64	4.84	2.88	10.3	91.76	58.26

TABLE IV
THE OVERALL PERFORMANCE OF THE TRAFFIC NETWORK AT DIFFERENT VOLUME UNDER CACC, CVSC, AND GLIDEPATH

V/C	Fuel Consumption			CO2 Emission			Average Speed			Average Waiting Time		
	Fuel(g/km)	Benefits (%)		CO2(g/km)	Benefits (%)		Speed(m/s)	Benefits (%)		Time(s)	Benefits (%)	
	CACC	CVSC	Glide	CACC	CVSC	Glide	CACC	CVSC	Glide	CACC	CVSC	Glide
0.2	66.17	1.86	1.59	144698.74	1.36	0.28	12.12	0.92	0.08	5.69	78.68	29.42
0.4	69.21	4.38	3.22	162164.42	3.53	0.67	11.98	1.32	0.65	9.55	72.51	38.31
0.6	72.02	9.55	6.63	161739.76	7.53	5.69	11.88	2.15	0.83	9.32	69.81	24.91
0.8	69.71	6.02	2.87	159839.33	4.65	2.08	11.43	1.45	0.21	10.10	65.75	22.79
1	78.39	5.78	1.34	208457.72	4.29	0.16	9.83	0.12	-0.38	18.48	67.58	50.79

TABLE V
THE OVERALL PERFORMANCE OF THE TRAFFIC NETWORK AT DIFFERENT OD CONDITIONS UNDER CACC, CVSC, AND GLIDEPATH

OD (WET:WEL:NSS:NSL)	Fuel Consumption			CO2 Emission			Average Speed			Average Waiting Time		
	Fuel(g/km)	Benefits (%)		CO2(g/km)	Benefits (%)		Speed(m/s)	Benefits (%)		Time(s)	Benefits (%)	
	CACC	CVSC	Glide	CACC	CVSC	Glide	CACC	CVSC	Glide	CACC	CVSC	Glide
1:1:1:1	69.71	6.02	2.87	159839.33	4.65	2.08	11.43	1.45	0.21	10.1	65.75	22.79
1:2:3:4	71.69	8.63	3.56	166769.01	7.01	3.37	10.86	6.68	1.66	12.12	75.59	32.25
1:4:1:4	75.77	14.36	7.49	182515.42	12.98	6.02	10.06	13.97	1.54	15.93	77.37	38.48

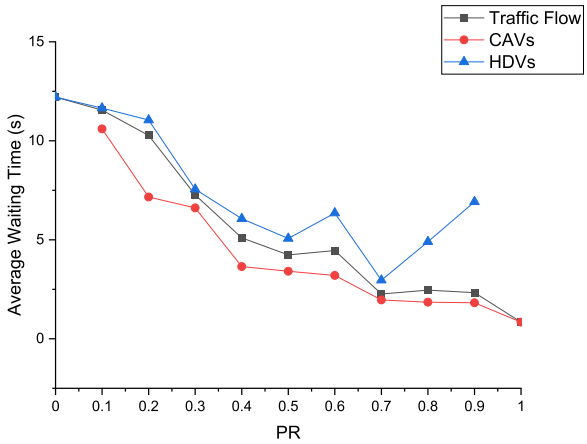

Fig. 13. The average vehicle waiting time with different PR.

improvement of the system is most obvious. It achieves 9% and 2% reduction in fuel consumption and the improvement in speed respectively. When the traffic flow is saturated, the performances of the three control methods are all reduced.

An unbalanced traffic volume simulation was also conducted, which compared the performance of three methods under different Origin-Destination (OD) conditions. Except that the volume in different directions is different, other experimental conditions are the same as the balancing volume experiment. The results are illustrated in Table V. The first row of Table V is the ratio of traffic flow in the four directions, which are west-east-through (WET), west-east-left turning (WEL), north-south-through (NST), north-south-left turning (NSL). The CVSC method has obvious advantages under the unbalanced traffic demand because the traffic signal timing plan is optimized according to the predicted delayed vehicle. When the demand in one direction increases significantly, the proposed CVSC method can still effectively improve the efficiency of the intersection more than 13% and reduce fuel consumption up to 14%.

VI. CONCLUSION AND FUTURE WORK

This paper proposed a coupled signal-vehicle control method for signalized intersection optimization in a mixed traffic environment. First, the fundamental diagram model of mixed traffic flow is derived from a combination of a set of car-following models. On the basis of this model, the traffic signal timing optimization and CAV eco-driving trajectory generation methods are proposed. For vehicles that cannot pass through the intersection during the green time of the current cycle, that is, delayed vehicles. An optimization function with the goal of minimizing all vehicles' delay time is set up. A set of green times for all phases is solved as the signal timing for the next control cycle. For the CAVs, the planned arrival time is calculated, considering the impact of the stop-start wave. The planned arrival time is involved in the trigonometric function algorithm to generate an eco-driving trajectory.

The results show that the proposed CVSC method can effectively improve the overall performance of traffic flow at signalized intersections in terms of fuel consumption, emissions, vehicle delay, and vehicle waiting time. In addition, it can perform well under moderate traffic flow conditions and adapt to unbalanced traffic demand. It is worth noting that the proposed CVSC method can be used not only at the intersection illustrated in this article, but also in other scenarios, as long as the input route model is adjusted. The reason is that the optimization function of I-TSC is based on structured upstream traffic data that is irrelevant to the static road parameters. In addition, this method can realize the seamless transfer from traditional traffic flow to fully automated traffic flow. When there are all HDVs in the environment, the CVSC system degenerates into a traffic signal adaptive optimization system. When all are CAVs, vehicles achieve passing through the intersection almost without stopping, because the average vehicle waiting time is close to 0.

For future work, the proposed method can be extended in a few important directions. This paper focused on the optimization of a single intersection and did not consider the impact of adjacent intersections. The optimization control method of the vehicle routing algorithm and multi-intersection signal coordination will be focused on the next step. Also, more complicated situations where there are different driving styles of drivers should be further studied.

REFERENCES

[1] D. Schrank, B. Eisele, and T. Lomax, "2019 urban mobility report," Texas A&M Transp. Inst., Tech. Rep. 01716050, 2019.
[2] S. A. F. Al-Arkawazi, "Measuring the influences and impacts of signalized intersection delay reduction on the fuel consumption, operation cost and exhaust emissions," *Civil Eng. J.*, vol. 4, no. 3, pp. 552–571, 2018.
[3] H. Marzbani, H. Khayyam, C. N. To, D. V. Quoc, and R. N. Jazar, "Autonomous vehicles: Autodriver algorithm and vehicle dynamics," *IEEE Trans. Veh. Technol.*, vol. 68, no. 4, pp. 3201–3211, Apr. 2019.
[4] X. Ma, M. Shahbakhti, and C. Chigan, "Connected vehicle based distributed meta-learning for online adaptive engine/powertrain fuel consumption modeling," *IEEE Trans. Veh. Technol.*, vol. 69, no. 9, pp. 9553–9565, Sep. 2020.
[5] S. Wei, D. Yu, C. L. Guo, L. Dan, and W. W. Shu, "Survey of connected automated vehicle perception mode: From autonomy to interaction," *IET Intell. Transp. Syst.*, vol. 13, no. 3, pp. 495–505, 2019.

[6] Q. Guo, L. Li, and X. J. Ban, "Urban traffic signal control with connected and automated vehicles: A. survey," *Transp. Res. Part C-Emerg. Technol.*, vol. 101, pp. 313–334, 2019.
[7] Z. Wang, Y. Bian, S. E. Shladover, G. Wu, S. E. Li, and M. J. Barth, "A survey on cooperative longitudinal motion control of multiple connected and automated vehicles," *IEEE Intell. Transp. Syst. Mag.*, vol. 12, no. 1, pp. 4–24, 2020.
[8] Z. Li, L. Elefteriadou, and S. Ranka, "Signal control optimization for automated vehicles at isolated signalized intersections," *Transp. Res. Part C-Emerg. Technol.*, vol. 49, pp. 1–18, 2014.
[9] P. B. Hunt, D. I. Robertson, R. D. Bretherton, and R. I. Winton, "Scoot-a traffic responsive method of coordinating signals," *Pub. Transp. Road Res. Lab.*, vol. 1014, 1981.
[10] P. R. Lowrie, "The sydney coordinated adaptive traffic system - principles, methodology, algorithms," in *Proc. Int. Conf. Road Traffic Signalling*, London, U.K., no. 207, 1982, pp. 130–137.
[11] Y. Du, W. ShangGuan, D. Rong, and L. Chai, "RA-TSC: Learning adaptive traffic signal control strategy via deep reinforcement learning," in *Proc. IEEE Intell. Transp. Syst. Conf.*, 2019, pp. 3275–3280.
[12] K.-L. A. Yau, J. Qadir, H. L. Khoo, M. H. Ling, and P. Komisarczuk, "A survey on reinforcement learning models and algorithms for traffic signal control," *ACM Comput. Surveys*, vol. 50, no. 3, p. 34, 2017.
[13] X. Liang, X. Du, G. Wang, and Z. Han, "A deep reinforcement learning network for traffic light cycle control," *IEEE Trans. Veh. Technol.*, vol. 68, no. 2, pp. 1243–1253, Feb. 2019.
[14] T. Wu *et al.*, "Multi-agent deep reinforcement learning for urban traffic light control in vehicular networks," *IEEE Trans. Veh. Technol.*, vol. 69, no. 8, pp. 8243–8256, Aug. 2020.
[15] H. Jiang, J. Hu, S. An, M. Wang, and B. B. Park, "Eco approaching at an isolated signalized intersection under partially connected and automated vehicles environment," *Transp. Res. Part C-Emerg. Technol.*, vol. 79, pp. 290–307, 2017.
[16] J. Ma, X. Li, F. Zhou, J. Hu, and B. B. Park, "Parsimonious shooting heuristic for trajectory design of connected automated traffic Part II: Computational issues and optimization," *Transp. Res. Part B-Methodological*, vol. 95, pp. 421–441, 2017.
[17] O. D. Altan, G. Wu, M. J. Barth, K. Boriboonsomsin, and J. A. Stark, "Glidepath: Eco-friendly automated approach and departure at signalized intersections," *IEEE Trans. Intell. Veh.*, vol. 2, no. 4, pp. 266–277, Dec. 2017.
[18] Z. Wang, G. Wu, and M. J. Barth, "Cooperative eco-driving at signalized intersections in a partially connected and automated vehicle environment," *IEEE Trans. Intell. Transp. Syst.*, vol. 21, no. 5, pp. 2029–2038, May 2020.
[19] J. Lee and B. Park, "Development and evaluation of a cooperative vehicle intersection control algorithm under the connected vehicles environment," *IEEE Trans. Intell. Transp. Syst.*, vol. 13, no. 1, pp. 81–90, Mar. 2012.
[20] A. A. Zaidi, B. Kulcsar, and H. Wymeersch, "Back-pressure traffic signal control with fixed and adaptive routing for urban vehicular networks," *IEEE Trans. Intell. Transp. Syst.*, vol. 17, no. 8, pp. 2134–2143, Aug. 2016.
[21] Y. Xu, D. Li, and Y. Xi, "A game-based adaptive traffic signal control policy using the vehicle to infrastructure (V2I)," *IEEE Trans. Veh. Technol.*, vol. 68, no. 10, pp. 9425–9437, Oct. 2019.
[22] B. Xu *et al.*, "Cooperative method of traffic signal optimization and speed control of connected vehicles at isolated intersections," *IEEE Trans. Intell. Transp. Syst.*, vol. 20, no. 4, pp. 1390–1403, Apr. 2019.
[23] L. Chai, B. Cai, W. S.Guan, J. Wang, and H. Wang, "Connected and autonomous vehicles coordinating approach at intersection based on space-time slot," *Transportmetrica*, vol. 14, no. 10, pp. 929–951, 2018.
[24] L. Chai, B. Cai, W. S.Guan, and J. Wang, "Connected and autonomous vehicles coordinating method at intersection utilizing preassigned slots," in *Proc. IEEE 20th Int. Conf. Intell. Transp. Syst.*, 2017, pp. 1–6.
[25] A. Talebpour and H. S. Mahmassani, "Influence of connected and autonomous vehicles on traffic flow stability and throughput," *Transp. Res. Part C-Emerg. Technol.*, vol. 71, pp. 143–163, 2016.
[26] F. Navas and V. Milanés, "Mixing V2V- and non-V2V-equipped vehicles in car following," *Transp. Res. Part C-Emerg. Technol.*, vol. 108, pp. 167–181, 2019.
[27] Z. Yao, R. Hu, Y. Wang, Y. Jiang, B. Ran, and Y. Chen, "Stability analysis and the fundamental diagram for mixed connected automated and human-driven vehicles," *Physica A-Stat. Mechanics Its Appl.*, vol. 533, 2019, Art. no. 121931.
[28] Q. Li, L. Chen, M. Li, S.-L. Shaw, and A. Nuchter, "A sensor-fusion drivable-region and lane-detection system for autonomous vehicle navigation in challenging road scenarios," *IEEE Trans. Veh. Technol.*, vol. 63, no. 2, pp. 540–555, Feb. 2014.
[29] M. Treiber, A. Hennecke, and D. Helbing, "Congested traffic states in empirical observations and microscopic simulations," *Phys. Rev. E*, vol. 62, no. 2, pp. 1805–1824, 2000.
[30] V. Milanes, S. E. Shladover, J. Spring, C. Nowakowski, H. Kawazoe, and M. Nakamura, "Cooperative adaptive cruise control in real traffic situations," *IEEE Trans. Intell. Transp. Syst.*, vol. 15, no. 1, pp. 296–305, Feb. 2014.
[31] V. Milanes and S. E. Shladover, "Modeling cooperative and autonomous adaptive cruise control dynamic responses using experimental data," *Transp. Res. Part C-Emerg. Technol.*, vol. 48, no. 48, pp. 285–300, 2014.
[32] J. Ploeg, E. Semsar-Kazerooni, G. Lijster, N. van de Wouw, and H. Nijmeijer, "Graceful degradation of cooperative adaptive cruise control," *IEEE Trans. Intell. Transp. Syst.*, vol. 16, no. 1, pp. 488–497, Feb. 2015.
[33] M. Behrisch, L. Bieker, J. Erdmann, and D. Krajzewicz, "Sumo - simulation of urban mobility an overview," in *Proc. SIMUL 3rd Int. Conf. Adv. Syst. Simul.*, 2011, pp. 55–60.
[34] S. Hausberger, M. Rexeis, M. Zallinger, and R. Luz, "Emission factors from the model PHEM for the HBEFA version 3," Inst. Intern. Combustion Engines and Thermodynamics, Tech. Rep. I-20/2009, 2009.

Yu Du (Member, IEEE) received the B.S. degree from Bejing Jiaotong University, Beijing, China, in 2012. She is currently working toward the Ph.D. degree with the School of Electronic and Information Engineering, Beijing Jiaotong University, studying the transportation information engineering and control. Her research interest focuses on cooperative vehicle and infrastructure system.

Wei ShangGuan (Member, IEEE) received the B.S., M.S., and Ph.D. degrees from Harbin Engineering University, in 2002, 2005, and 2008, respectively. From 2013 to 2014, he was an Academic Visitor with the University College London. He is currently a Professor and a Supervisor for Ph.D's studies with the School of Electronic and Information Engineering, Beijing Jiaotong University. His research interests include system modeling, simulation and testing, integrated navigation, intelligent transportation system, cooperative vehicle infrastructure system of China (CVIS-C), and train control system.

Linguo Chai (Member, IEEE) recrived the B.S, M.S, and Ph.D degrees from Beijing Jiaotong University in 2010, 2012, and 2018, respectively. He is currently a Lecturer with the School of Electronic and Information Engineering, Beijing Jiaotong University. From 2016 to 2017, he was a Visiting Scholar with PATH, UC, Berkeley. His researches concentrate on vehicle operational control of CVIS, CVIS modeling and simulation, simulation of train control system.